ELSEVIER

Journal of Organometallic Chemistry 526 (1996) 1–14

Journal of Organometallic Chemistry

Synthesis and characterization of polyaromatic azine derivatives of $(\eta^5\text{-}C_5H_5)Fe(CO)_2$ and $(\eta^5\text{-}C_9H_7)Fe(CO)_2$: X-ray crystal structures of 4-[(η^5-cyclopentadienyl)irondicarbonyl]-7-chloroquinoline, 2-[(η^5-cyclopentadienyl)irondicarbonyl]-3-chloroquinoxaline, and 2-[(η^5-indenyl)irondicarbonyl]-3-chloroquinoxaline

Allen D. Hunter [a,*], Roxton Chukwu [b], Bernard D. Santarsiero [b,1], Simon G. Bott [c,1] Jerry L. Atwood [d]

[a] *Department of Chemistry, Youngstown State University, Youngstown, OH 44555-3663, USA*
[b] *Department of Chemistry, University of Alberta, Edmonton, Alta. T6G 2G2, Canada*
[c] *Department of Chemistry, University of North Texas, Denton, TX 76203, USA*
[d] *Department of Chemistry, University of Alabama, Tuscaloosa, AL 35487, USA*

Received 21 March 1995; revised 6 March 1996

Abstract

The synthesis and characterization of 14 monometallic derivatives of quinoline, quinoxaline, quinazoline and tetraazolo(1,5-A)quinoline and a bimetallic derivative of quinoxaline are reported. These species were prepared in 11 to 88% isolated yields by metathesis reactions between NaFp or NaFp^1 (where Fp = $(\eta^5 - C_5H_5)Fe(CO)_2$ and Fp^1 = (η^5 – indenyl)$Fe(CO)_2$) and the appropriate chlorine substituted polyaromatic azines. These reactions are highly regioselective and generally produce a single organometallic product having the organometallic substituent(s) bonded to the more highly activated azine ring. The structures of three representative examples were confirmed by their X-ray crystal structures, which are reported for the title complexes 4-[(η^5-cyclopentadienyl)irondicarbonyl]-7-chloroquinoline ($C_{16}H_{10}ClFeNO_2$; $a = 7.608(1)$ Å, $b = 12.006(1)$ Å, $c = 15.664(1)$ Å, $V = 1431$ Å^3; orthorhombic; $P2_12_12_1$; $Z = 4$), 2-[(η^5-cyclopentadienyl)irondicarbonyl]-3-chloroquinoxaline ($C_{15}H_9ClFeN_2O_2$; $a = 15.291(3)$ Å, $b = 6.561(2)$ Å, $c = 14.541(4)$ Å, $\beta = 106.891(21)°$, $V = 1395.9$ Å^3; monoclinic; $P2_1/c$; $Z = 4$), and 2-[(η^5-indenyl)irondicarbonyl]-3-chloroquinoxaline ($C_{19}H_{11}ClFeN_2O_2$; $a = 19.131(2)$ Å, $b = 6.688(1)$ Å, $c = 13.515(2)$ Å, $\beta = 101.569(11)°$, $V = 1694.1$ Å^3; monoclinic; $P2_1/c$; $Z = 4$). The bimetallic quinoxaline derivative 2,3-[$(C_5H_5)_2Fe_2(CO)_4$]-quinoxaline has *ortho*-substituted organometallic groups and the spectroscopic data suggest that it has an unusual structure in solution, perhaps involving bridging cyclopentadienyl and carbonyl ligands.

Keywords: Iron; Cyclopentadienyl; Heterocyclics; Crystal structure; Azines; Carbonyl

1. Introduction

We have recently been studying organometallic complexes in which two or more metal-containing fragments are bridged by arene or heteroarene ligands (i.e. 1,4-$C_6H_4(Mn(CO)_5)_2$, (η^6-1,4-$C_6H_4(OMe)Fp$) $Cr(CO)_3$, and 2-chloro-4,6-Fp_2-pyrimidine, where Fp = $(\eta^5 - C_5H_5)Fe(CO)_2$) [1–9] since such compounds serve as models for the repeating units in related organometallic polymers [10–14]. Increasing the number of fused aromatic rings in the bridging groups of such materials (i.e. going from 1,4-C_6H_4 to 1,4-$C_{10}H_6$ to 9,10-$C_{14}H_8$) [8] is expected to increase the degree of intermetallic conjugation in complexes having two metal centers σ-bonded to the rings, as has been demonstrated for conjugated organic polymers [15]. To explore the magnitude, if any, of this effect for azine bridged materials and to see how the addition of a fused ring would affect their structures and chemical reactivity, we have studied Fp substituted derivatives of fused heteroarene ligands [16]. Although we were able to synthesize a series of *meta*-substituted bimetallic model com-

* Corresponding author.
[1] Present address: Molecular Structure Corp., 3200 Research Forest Drive, The Woodlands, TX 77381-4238, USA.

PII S0022-328X(96)06337-1

plexes (e.g. 2-methylmercapto-4,6-bis((η⁵-cyclopentadienyl)irondicarbonyl)pyrimidine), we were unsuccessful in our attempts to prepare the related *para*-substituted bimetallic model compounds (e.g. 3,6-bis((η⁵-cyclopentadienyl)irondicarbonyl)pyridazine) [1,2,16]. We were therefore particularly surprised that the reaction of 2,3-dichloroquinoxaline with two equivalents of NaFp produced a bimetallic material having unexpectedly complex spectroscopic properties and apparently having *ortho*-substituted metal centers, since all previous attempts to prepare the sterically crowded *ortho*-derivatives have met with failure [1,2,4–9]. We are also interested in the structural and electronic similarities between polyaromatic azine derivatives of iron and analogous organic compounds, since many of these are natural products and/or are known to exhibit biological activities in biomedical or agricultural applications (e.g. adenine, caffeine, chloroquine, and tetraazolo⟨1,5-A⟩quinoline) [17–22].

In this paper, we report the complete results of our efforts to synthesize fused ring heterocyclic derivatives of iron, including their spectroscopic characterizations and X-ray crystallographic studies of three representative examples.

2. Experimental

Unless otherwise noted, all reactions and subsequent manipulations were performed under anaerobic and anhydrous conditions. General procedures routinely employed in these laboratories have been described in detail previously [1,5,6]. The chemicals used were of reagent grade or comparable purity, and where necessary were purified before use and had their purity ascertained by elemental analyses and/or other suitable methods [23,24]. The heterocyclic starting materials for these syntheses were purchased from the Aldrich* chemical company or were supplied by DowElanco [2]. Solvents used were dried and deaerated by standard procedures and stored under N_2 or Ar [1,5,6,23,24]. Unless specified otherwise, the chemical reactions described below were effected at ambient temperatures. The Fp_2, and Fp_2^* (where $Fp = (\eta^5 - C_5H_5)Fe(CO)_2$ and $Fp^* = (\eta^5 - \text{indenyl})Fe(CO)_2$) used in these syntheses were prepared and purified by standard procedures [25,26]. In particular, the Fp_2^* used in this work was prepared in 45% yield by refluxing $Fe(CO)_5$ and indene in heptane for 16 h [25,26]. Infrared spectra were recorded on a Pye Unicam PU9522 infrared spectrophotometer calibrated with the 1601 cm^{-1} band of polystyrene. ^1H and ^{13}C NMR spectra were recorded on a Bruker WH-300 spectrometer. The ^1H and ^{13}C NMR chemical shifts are reported in parts per million downfield from external Me_4Si.

2.1. Preparation of the mono-substituted fused heterocyclic complexes of Fp

All these complexes were synthesized in a similar manner, the synthesis of 2-[(η⁵-cyclopentadienyl) irondicarbonyl]-3-chloroquinoxaline **10** being described as a representative example.

An excess of solid sodium amalgam (20.0 g, 20.0 mmol Na) [4] was placed in a 200 ml three-necked flask equipped with a side arm and the flask was thoroughly flushed with dinitrogen. (*Caution*: mercury is a volatile toxic substance and should therefore be handled with care, taking appropriate precautions.) The amalgam was liquified by addition of a few drops of mercury and then THF (75 ml) and Fp_2 (0.86 g, 2.45 mmol) were added. The resultant dark red solution was stirred vigorously for 45 min to produce an orange solution containing NaFp. The excess amalgam was then drained through the side arm on the reaction flask. A solution of the substrate, 2,3-dichloroquinoxaline (0.98 g, 4.9 mmol), was made in a three-necked flask and cooled to around −78 °C, and then the NaFp solution prepared earlier was filtered through a bed of Celite supported on a fritted funnel into this solution. The cooling source was removed after 30 min, and the solution allowed to warm to room temperature over 3 h. The solution was taken to dryness in vacuo, and then the product was purified by column chromatography (Florisil packed 2.5 × 14 cm^2 column) in air. The first (purple) band was eluted with CH_2Cl_2/hexane (1:1). It was identified as Fp_2 by its IR spectrum and was discarded. The second band (yellow) was eluted with CH_2Cl_2 and the eluant was concentrated to yield 39% (0.64 g, 1.9 mmol) of orange crystals of $C_{15}H_9ClFeN_2O_2$, **10**.

The non-optimized yields, analytical, mass spectral, IR and NMR data for all of the complexes isolated in this work are recorded in Tables 1 and 2. Each of the complexes listed in Tables 1 and 2 was prepared similarly from the appropriate chlorine substituted heterocyclic reagent (in each case this material has a chlorine atom in the position in which the Fp group ends up in the final product, i.e. 2-chloroquinoline, 4-chloroquinoline, 4-chloro-8-fluoroquinoline, 4,7-dichloroquinoline, 4,5,7-trichloroquinoline, 4-chlorotetraazolo⟨1,5-A⟩quinoline, 4-chloro-8-fluoroquinazoline, 2-chloro-3-methylquinoxoline, 2,3-dichloroquinoxoline, 2,3,6-trichloroquinoline, 2,5,6-trichloroquioxaline). The analogous reactions involving the reagents 3-chloro-7-methoxy-1,2,4-benzotriazine-1-oxide, 2-chloro-3-phenylquinoxaline, and 1,4-dichlorophthalazine, which were carried out in a similar manner, produced Fp_2 as the only detected organometallic product.

[2] DowElanco, Discovery Research, PO Box 708, Greenfield, IN, USA.

Table 1
Yields, analytical, mass spectral and infrared data for the complexes

Complex [a]	Yield (%)	Anal. data						Low-resolution mass spectral data P^+, m/z [b]	Infrared data ν_{CO} (CH_2Cl_2, cm^{-1}) [c]
		C		H		N			
		Calc.	Found	Calc.	Found	Calc.	Found		
2-Fp-quinoline, **1** [d]	11	62.98	61.61	3.63	4.17	4.59	4.54	277 [e]	2022 (s), 1968 (s)
4-Fp-quinoline, **2** [d]	15	62.98	63.28	3.63	4.42	4.59	4.51	305	2022 (s), 1972 (s)
4-Fp-8-F-quinoline, **3**	46	59.45	59.78	3.12	3.36	4.33	4.76	323	2024 (s), 1974 (s)
4-Fp-7-Cl-quinoline, **4**	60	56.58	56.15	2.97	2.95	4.12	4.05	339	2024 (s), 1973 (s)
4-Fp-5,7-Cl_2-quinoline, **5**	38	51.38	51.42	2.43	2.45	3.76	4.37	345 [e]	2024 (s), 1974 (s)
5-Fp-tetraazalo⟨1,5-A⟩quinoline, **6**	49	53.89	53.78	3.02	2.92	16.82	17.53	318 [e]	2028 (s), 1976 (s)
4-Fp-8-F-quinazoline, **7**	56	55.59	55.85	2.80	2.68	8.65	9.02	324	2031 (s), 1977 (s)
2-Fp-3-Me-quinoline, **8**	53	60.03	59.47	3.78	3.90	8.76	8.49	320	2026 (s), 1970 (s)
2-Fp-3-Cl-quinoxaline, **10**	59	52.90	53.24	2.66	2.78	8.23	8.18	340	2036 (s), 1983 (s)
3-Fp-2,7-Cl_2-qinoxaline, 2-Fp-3,7-Cl_2-qinoxaline, **11a and 11b** [f]	76	48.08	47.74	2.15	2.25	7.48	7.09	374	2034 (s), 1980 (s)
2-Fp-6,7-Cl_2-qinoxaline, **12**	88	48.08	47.60	2.15	2.15	7.48	7.25	374	2026 (s), 1977 (s)
2-Fp‡-3-Cl-quinoxaline, **13**	70	57.83	57.98	2.81	2.99	7.10	7.14	362 [e]	2027 (s), 1977 (s)
2,3-{$(C_5H_5)_2Fe_2(CO)_4$}-quinoxaline $\cdot 0.5CH_2Cl_2$, **14**	26	51.60	52.04	2.90	3.10	5.34	5.49	482 [g]	2038 (s), 1992 (s), 1928 (s)

[a] Where Fp = $(\eta^5-C_5H_5)Fe(CO)_2$ and Fp‡ = $(\eta^5$ – indenyl$)Fe(CO)_2$.
[b] Probe temperature 150–280 °C. Assignments involve the most abundant naturally occurring isotopes (e.g. ^{35}Cl, ^{56}Fe). All ions displayed peak patterns attributable to the expected isotopomers of the non-solvated species, see text.
[c] Abbreviations w (weak), m (medium), s (strong), sh (shoulder), v (very), br (broad).
[d] This complex was characterized spectroscopically but was not obtained in an analytically pure form, see text.
[e] No parent ion observed in the low resolution mass spectrum, heaviest ion observed as P^+-CO.
[f] Solid isolated is a mixture of isomers.
[g] Assignments confirmed by high resolution mass spectra.

2.2. Preparation of the disubstituted fused heterocyclic complexes of Fp

An orange solution of NaFp (10.1 mmol) in THF (90 ml) prepared as described above was filtered into a cold (around −78 °C) solution of the substrate, 2,3-dichloroquinoxaline (1.00 g, 5.0 mmol) in THF (75 ml), and the mixture was stirred at this temperature for about20 min. An IR spectrum of the solution at this stage showed carbonyl peaks at 2030 (s), 1994 (sh), 1976 (s), 1954 (sh), and 1784 (s) cm^{-1}. The cooling source was removed, and the solution was allowed to warm to ambient temperature over 3 h, and an IR spectrum showed a new shoulder at 1932 cm^{-1}. An air cooled reflux condenser was attached to the flask, and the mixture was refluxed for 2 days at which point the peak at 1932 cm^{-1} became more pronounced. The solution was taken to dryness in vacuo, and the compound purified by column chromatography under an N_2 atmosphere (Florisil column, 2.5 × 14 cm^2). The first band (red) eluted with CH_2Cl_2 was shown by IR to contain Fp_2 as well as some of the mono-substituted complex $C_{15}H_9ClFeN_2O_2$, **10**. The second band (yellow) eluted with CH_2Cl_2 was shown to be the mono-substituted complex **10**, by comparison with an authentic sample (approximately 25% yield by IR). The third band (dark red) was eluted with THF and identified as the desired product. This last eluant was taken to dryness in vacuo and then dissolved in CH_2Cl_2 (30 ml). The mixture was filtered and the filtrate was again taken to dryness. The resulting solid was washed with cold (−9 °C) heptane (4 × 5 ml) and dried in vacuo to yield 26% (0.64 g, 13.3 mmol) of the dark red product $C_{22}H_{14}Fe_2N_2O_4 \cdot 0.5CH_2Cl_2$, **14**.

The reaction of 2,3,6,7-tetrachloroquinoxaline with two equivalents of NaFp proceeded similarly, but the desired product, $C_{22}H_{12}Cl_2Fe_2N_2O_4$, **15**, was not isolated in an analytically pure form and was therefore only characterized spectroscopically. IR ν_{CO} (CH_2Cl_2) 2040 (s), 1994 (s), and 1934 (s) cm^{-1}. Low-resolution mass spectrum m/z 522, 466 and 438 (P^+-nCO, n = 1, 3 and 4). The reaction of 2,3-dichloroquinoxaline with 2 equivalents of NaFp‡ apparently did not produce the desired bimetallic product $C_{30}H_{18}Cl_2Fe_2N_2O_4$, **16**, since no spectroscopic evidence consistent with bimetallic species was observed in the reaction mixture.

2.3. Isolation of the monosubstituted byproduct, complex 9, from the purification procedure for compound 14

In an attempt to purify disubstituted product **14** via column chromatography on Florisil, immediate elution of the desired product was, on one occasion, not carried out. The disubstituted product was left on the column exposed to air for 2 days, and the chromatography was then completed with two major bands being eluted. The first purple band was identified by IR as containing mainly the Fp_2 starting material as well as some traces

Table 2
^1H and ^{13}C NMR data for the complexes (δ in ppm; $(CD_3)_2SO$)

Complex [a]	^1H NMR [b] (Hz)		^{13}C NMR [b] (Hz)			
	Cp[‡]	Azine and substituents	Cp[‡]	azine		
				X–C	H–C	Fe–CO
1	5.18	7.25–7.90(6H)	86.77	188.54 [c]	137.7 128.51 128.02 127.71 127.42 123.78	8216.01
2	5.25	7.50–8.20(6H)	86.12	[c]	145.08 141.05 133.35 129.85 127.60 124.77	216.00
3	5.28 (s,5H)	8.18 (d, 1H, J = 4.5) 7.98 (d, 1H, J = 8) 7.95 (d, 1H, J = 4.5) 7.38–7.54 (m, 2H)	87.19	170.69 (C4) 157.46 [C8, 254] 142.77 136.76 [16] 111.58 [35]	144.70 141.93 129.37 [4–9] 124.16 [15]	215.75
4	5.27	8.18 (d, 2H, J = 9.1) 8.15 (d, 1H, J = 4.5) 7.89 (d, 1H, J = 4.5) 7.85 (d, 1H, J = 2.3) 7.52 (dd, 1H, J = 2.3, 9.1)	87.16	170.94 (C4) 147.26 (C7) 139.84 132.16	145.83 141.42 135.51 128.18 125.20	215.72
5	5.35 (s, 5H)	8.20 (d, 1H, J = 4.5) 8.06 (d, 1H, J = 4.5) 7.86 (d, 1H, J = 2.2) 7.70 (d, 1H, J = 2.2)	88.59	[c] 165.98 127.59	144.51 143.27 129.25	215.02
6	5.34 (s, 5H)	8.33 (dd, 1H, J = 8, 1) 8.44 (dd, 1H, J = 8, 1) 8.24 (s, 1H) 7.86 (ddd, 1H, J = 8, 7, 1) 7.77 (ddd, 1H, J = 8, 7, 1)	87.42	166.40 (C7) 144.07 133.65 128.09	135.34 128.85 127.12 125.74 116.09	215.53
7	5.26 (s, 5H)	8.70 (s, 1H) 8.03 (m, 1H) 7.62 (m, 2H) 135.08 [18–22]	87.16	216.24 156.56 [255] 149.96 15.81 [35]	148.99 128.64[4–9] 125.76 [15]	214.93
8	5.27 (s, 5H)	7.78 (m, 2H) 7.53 (m, 2H) 2.71 (s, 3H, CH_3)	87.34	189.51 (C2) 161.84 (C3) 142.06	128.26 127.97 127.25	215.79
10 [d]	5.25 (s, 5H)	7.89 (dd, H_A, J_{AC} = 12, J_{AD} = 2) 7.82 (dd, H_B, J_{BD} = 15, J_{BC} = 3)) 7.69 (ddd, H_C, J_{CD} = 14) 7.58 (ddd, Hd)	87.31	189.96 (C2) 158.57 (C3) 141.71 137.46	129.09 128.05 127.73 12.37	214.90
11 [e, g]	5.27 (s, 5H)	7.91 (s, 1H) 7.85 (d, 1H, J = 9) 7.62 (d, 1H)	87.35	193.55 (C2) 158.96 141.37 136.13 133.23	129.69 128.46 126.20	214.64
12	5.33 (s, 5H)	8.75 (s, 1H) 8.12 (s, 1H) 8.04 (s, 1H)	86.93	193.85 (C2) 142.76 137.51 131.06 128.43	157.70 130.07 128.43	214.83
13	7.59 (m, 2H)	7.80 (m, 2H) 7.17 (m, 2H) 5.96 (d, 2H, J = 3) 5.33 (t, 1H, J = 3)	128.30 (2C–H) 7.66 (m, 2H)	188.44 (C2) 124.80 (2C–H) 104.64 (2C) 95.33 (1C–H) 76.04 (2C–H)	129.09 157.73 (C3) 141.92 137.17	215.00 127.99 127.63 127.17

Table 2 (continued)

Complex [a]	^{1}H NMR [b] (Hz)		^{13}C NMR [b] (Hz)			
	Cp'	Azine and substituents	Cp'	azine		
				X–C	H–C	Fe–CO
14 [d,h]	5.22 (s, 5H)	7.98 (dd, H_A, J_{AD} = 8, J_{AC} = 1)	87.81	211.27	131.06	289.90
	4.74 (s, 5H)	7.93 (dd, H_B, J_{AC} = 8, J_{BD} = 1)	82.86	160.34	130.29	219.16
		7.79 (ddd, H_C, J_{CD} = 6)		143.96	126.63	214.12
		7.63 (ddd, H_D)		138.54	126.51	213.97

[a] Where Cp' = $\eta^5 - C_5H_5$ for all complexes except **13** for which it equals η^5-indenyl.
[b] ^{1}H, ^{13}C and ^{19}F NMR were measured at 300.135, 75.469, and 376.503 MHz respectively. J_{CF} values are reported in square brackets.
[c] The positions of some of these resonances could not be unambiguously assigned.
[d] ^{1}H NMR assignments confirmed by homonuclear decoupling experiments.
[e] Major isomer.
[f] ^{1}H NMR (CD_2Cl_2) 7.91 (d, 1H, J = 2), 7.76 (d, 1H, J = 9), 7.48 (dd, 1H, J = 9, 2), 5.04 (s, 5H, C_5H_5) ppm for the major isomer and 7.85 (d, 1H, J = 9), 7.80 (d, 1H, J = 2) and 7.57 (dd, 1H, J = 9, 2) ppm for the minor isomer (20% of total); the Cp signals of the two isomers overlap.
[g] ^{13}C NMR ($(CD_3)_2SO$) 214.70 (*C*O), 129.54 (*C*-H), 129.16 (*C*-H) and 126.53 (*C*-H) ppm for the minor isomer, the Cp signals overlap.
[h] Signals due to CH_2Cl_2 of solvation are observed in $(CD_3)_2SO$ at 5.76 ppm in the ^{1}H NMR and at 54.87 ppm in the ^{13}C NMR for complex **14**.

of the monosubstituted complex **10**. The second major band (dark purple) contained a new product whose IR spectrum showed carbonyl bands in CH_2Cl_2 at 2028 (s), 1973 (s) cm^{-1}. Analysis of the material by MS showed that one of the Fp groups had been replaced by a H atom. This new complex, 2-Fp-quinoxaline **9**, was further purified by chromatography to exclude all of the Fp_2 starting material. Subsequent to this, complex **9** was obtained by deliberately pumping air through a Florisil column loaded with **14** in CH_2Cl_2. Unfortu-

Table 3
Summary of crystal data and intensity collection for complexes **4**, **10**, and **13**

Parameter	**4**	**10**	**13**
Formula	$C_{16}H_{10}ClFeNO_2$	$C_{15}H_9ClFeN_2O_2$	$C_{10}H_{11}ClFeN_2O_2$
Formula weight	339.57	340.55	390.61
Crystal dimensions (mm)	0.09 × 0.09 × 0.11	0.36 × 0.42 × 0.55	0.21 × 0.36 × 0.55
Space group	$P2_12_12_1$	$P2_1/c$	$P2_1/c$
Crystal system	orthorhombic	monoclinic	monoclinic
a (Å)	7.608(1)	15.291(3)	19.131(2)
b (Å)	12.006(1)	6.561(2)	6.688(1)
c (Å)	15.664(1)	14.541(4)	13.515(2)
β (°)	—	106.891(21)	101.569(11)
V (Å^3)	1431	1395.9	1694.1
Z	4	4	4
Calc. density (g cm^{-3})	1.582	1.620	1.531
Abs. coeff. (cm^{-1})	12.46	12.75	5.50
Diffractometer	Enraf-Nonius CAD4	Enraf-Nonius CAD4	Enraf-Nonius CAD4
Radiation	Mo K_α (λ = 0.7107 Å)	Mo K_α (λ = 0.7107 Å)	Mo K_α (λ = 0.7107)
Monochromator/filter	incident beam, graphite crystal	incident beam, graphite crystal	incident beam, graphite crystal
Take-off angle (°)	2.8	3.00	3.00
Detector aperture (mm)	3.00 + tan θ horiz. × 4.0 vert.	2.40 horiz. × 4.0 vert.	2.40 horiz. × 4.0 vert.
Crystal-to-detector distance (mm)	205	205	205
Scan type	θ–2θ	θ–2θ	θ–2θ
Scan width	0.80 + 0.35tan θ	1.00 + 0.347tan θ	0.80 + 0.347tan θ
Scan rate (° min^{-1})	0.8–8.0	2.0	2.2–6.7
2θ range (°)	2–50	2–60	2–50
Data collection index range	h, k, l	$\pm h$, k, $\pm l$	h, k, $\pm l$
Number of reflections	1521 total	4400 total, averaged	5048 total, averaged
Number of significant reflections in refinement	1235 ($F > 6\sigma(F)$)	2915($I > 3\sigma_I$)	2958 ($I > 2\sigma_I$)
Observations/variables ratio	1235/190	2915/190	2958/226
Agreement factor R_1, R_2, GOF	0.0450, 0.0499, 1.42	0.037, 0.051, 1.81	0.042, 0.053, 1.59
Corrections applied	ψ scans	empirical absorption correction	empirical absorption correction
Data collection temperature	25 °C	−20 °C	25 °C

Table 4
Positional and equivalent isotropic Gaussian ($Å^2$) parameters for complex **4** [a,b]

Atom	x	y	z	U_{eq}
Fe	0.3490(2)	0.4061(1)	0.11883(7)	0.045(6)
Cl	0.3651(5)	1.0118(2)	0.0462(2)	0.081(14)
O(1)	0.0264(8)	0.2816(6)	0.0856(4)	0.080(17)
C(1)	0.152(1)	0.3307(7)	0.1005(5)	0.057(5)
O(2)	0.359(1)	0.4599(6)	−0.0607(4)	0.080(18)
C(2)	0.360(1)	0.4410(7)	0.0108(5)	0.054(6)
C(11)	0.211(1)	0.5429(7)	0.1481(5)	0.043(6)
C(12)	0.063(1)	0.5310(7)	0.2013(5)	0.055(3)
C(13)	−0.032(1)	0.6236(8)	0.2255(6)	0.062(9)
N(14)	−0.0008(9)	0.7267(7)	0.2028(5)	0.062(13)
C(15)	0.177(1)	0.8532(7)	0.1261(5)	0.053(7)
C(16)	0.326(1)	0.8754(7)	0.0776(5)	0.055(10)
C(17)	0.435(1)	0.7916(8)	0.0510(5)	0.056(8)
C(18)	0.402(1)	0.6841(7)	0.0745(5)	0.051(2)
C(19)	0.145(1)	0.7427(6)	0.1513(4)	0.047(5)
C(20)	0.255(1)	0.6537(6)	0.1240(5)	0.044(4)
C(101)	0.411(1)	0.341(1)	0.2394(7)	0.083(31)
C(102)	0.495(2)	0.445(1)	0.2294(7)	0.080(9)
C(103)	0.607(1)	0.438(1)	0.1598(8)	0.087(36)
C(104)	0.594(1)	0.326(1)	0.1271(9)	0.099(32)
C(105)	0.472(2)	0.268(1)	0.1768(9)	0.099(39)

[a] Estimated standard deviations, in parentheses, refer to the last significant digit.

[b] The equivalent isotropic displacement parameter U_{eq} is $(1/3)\sum_{i=1}^{3} r_i^2$, where the r_i ($Å^2$) are the root-mean-square amplitudes of the displacement.

nately, complex **9** was not obtained in analytically pure form and was therefore only characterized spectroscopically. IR (CH_2Cl_2) ν_{CO} 2028 (s), 1973 (s) cm^{-1}. Low-resolution mass spectrum m/z 306 (P^+). ^1H NMR ($(CD_3)_2SO$) 7.9 (br), 5.2 (br). ^{13}C NMR ($(CD_3)_2SO$) 86.47 (s, C_5H_5), 126.44, 127.13, 128.21 and 128.71 (s, C_5, C_6, C_7 and C_8), 138.12 and 144.37 (s, C_9 and C_{10}), 156.30 (s, C3), 188.24 (s, C2), 214.93 (Fe*C*O).

A similar side reaction was observed in the preparation of complex **15**, yielding complex **12**.

Table 5
Positional ($\times 10^4$) and equivalent isotropic Gaussian ($Å^2 \times 10^2$) parameters for complex **10** [a,b]

Atom	x	y	z	U_{eq}
Fe	1721.2(2)	1924.3(5)	1477.0(2)	3.131(7)
Cl	1085.9(4)	4168(1)	3356.8(4)	5.59(2)
O21	0(1)	4127(3)	995(1)	6.25(7)
O22	2371(1)	4082(3)	53(1)	5.98(6)
N1	3253(1)	4389(3)	2402(1)	3.66(5)
N4	2708(1)	5629(3)	3987(1)	3.92(5)
C2	2430(1)	3881(3)	2440(1)	3.22(5)
C3	2187(1)	4633(4)	3272(1)	3.43(5)
C5	4185(2)	7152(4)	4689(2)	4.98(8)
C6	5037(2)	7618(4)	4622(2)	5.68(9)
C7	5285(2)	7112(4)	3793(2)	5.73(9)
C8	4700(2)	6070(4)	3064(2)	5.10(8)
C9	3828(1)	5497(4)	3128(2)	3.82(6)
C10	3570(1)	6080(4)	3938(2)	3.76(6)
C11	1885(2)	−1010(4)	946(2)	5.46(8)
C12	2628(2)	−546(4)	1778(2)	5.86(9)
C13	2258(2)	−270(4)	2551(2)	5.24(8)
C14	1313(2)	−508(4)	2203(2)	5.03(7)
C15	1084(2)	−982(4)	1214(2)	5.07(8)
C21	686(2)	3304(4)	1203(2)	4.10(7)
C22	2111(2)	3232(4)	607(2)	4.04(6)

[a] Estimated standard deviations, in parentheses, refer to the last significant digit.

[b] The equivalent isotropic displacement parameter U_{eq} is $(1/3)\sum_{i=1}^{3} r_i^2$, where the r_i ($Å^2$) are the root-mean-square amplitudes of the displacement.

Table 6
Positional ($\times 10^4$) and equivalent isotropic Gaussian ($Å^2 \times 10^2$) parameters for complex **13** [a]

Atom	x	y	z	U_{eq}
Fe	2978.3(2)	3182.5(6)	7842.5(3)	4.54(1)
Cl	1971.3(5)	1495(2)	9537.7(6)	7.73(3)
O21	3788(1)	738(4)	9453(2)	8.63(9)
O22	3512(1)	1244(4)	6211(2)	6.95(8)
N1	1937(1)	723(3)	6625(2)	4.57(7)
N4	1152(1)	−332(4)	8080(2)	5.38(7)
C2	2150(1)	1366(4)	7553(2)	4.31(8)
C3	1724(1)	733(5)	8276(2)	5.13(9)
C5	314(2)	−2102(5)	6826(2)	6.1(1)
C6	105(2)	−2751(5)	5853(2)	6.5(1)
C7	512(2)	−2264(5)	5129(2)	6.6(1)
C8	1114(2)	−1141(5)	5383(2)	5.78(9)
C9	1334(1)	−431(4)	6372(2)	4.41(8)
C10	933(1)	−949(4)	7097(2)	4.59(8)
C11	3313(2)	6126(4)	7416(3)	6.4(1)
C12	2558(2)	5763(5)	7069(3)	7.3(1)
C13	2259(2)	5493(5)	7935(3)	6.8(1)
C14	2797(2)	5535(5)	8802(2)	6.5(1)
C15	3453(2)	5979(4)	8485(2)	5.7(1)
C16	4157(2)	6256(5)	9050(3)	7.3(1)
C17	4677(2)	6700(6)	8557(3)	8.9(2)
C18	4555(2)	6834(5)	7508(3)	9.7(1)
C19	3892(2)	6531(5)	6924(3)	8.5(1)
C21	3454(2)	1660(4)	8816(2)	5.67(9)
C22	3295(1)	1985(4)	6854(2)	5.11(9)

[a] Estimated standard deviations, in parentheses, refer to the last significant digit.

[b] The equivalent isotropic displacement parameter U_{eq} is $(1/3)\sum_{i=1}^{3} r_i^2$, where the r_i ($Å^2$) are the root-mean-square amplitudes of the displacement.

2.4. X-ray crystallographic characterization of complexes 4, 10, and 13

Crystals suitable for X-ray examination were grown from CH_2Cl_2/hexanes at −15 °C. They were mounted on glass fibers and optically centered in the X-ray beam on an Enraf-Nonius CAD4 automated diffractometer. Data collection and structure solution parameters are given in Table 3. Data were corrected for Lorentz and polarization effects and also for absorption (via empirical Ψ scans [27–29] for **4** (max/min correction 1.0/0.81) and via the method of Walker and Stuart [30] for **10** and **13**) (see Supplementary material available). Details of the usual procedures used in our laboratories have been published elsewhere [1,27].

Structure solution proceeded in a routine fashion for all three compounds utilizing SHELXS-86 and SHELX-76 for **4** [27–29] and the SDP structure solution package for compounds **10** and **13** [30]. All non-hydrogen atoms were treated with anisotropic displacement parameters. All hydrogen atoms were generated in idealized positions and included in the model as "riding" on the attached atom with isotropic displacement parameters constrained to be 1.2 times that of the attached atom. Final fractional atomic coordinates and equivalent isotropic displacement parameters are given in Table 4, Table 5, and Table 6 for compounds **4**, **10**, and **13** respectively (see Supplementary material available).

Many attempts to grow crystals of compound **14** suitable for X-ray diffraction analysis were made. However, inspection under a polarizing microscope and/or rotation photographs and attempts to obtain an acceptable unit cell (on the Siemens P4 diffractometer located at the Youngstown State University Structure Center) indicated that in each case the crystals were badly twinned.

3. Results and discussion

3.1. Synthesis of the complexes

The ease of nucleophilic attack at heteroaromatic rings is enhanced for organic nucleophiles by progressive substitution of the ring carbon atoms by nitrogen atoms (e.g. pyrimidines are more reactive than pyridines) and by fusing a benzene ring to a halide substituted heterocyclic ring (e.g. 2-chloroquinoline is 1000 times more reactive than 2-chloropyridine) [31]. We observe similar trends for the reactions of one equivalent of NaFp (where $Fp = (\eta^5 - C_5H_5)Fe(CO)_2$) with fused

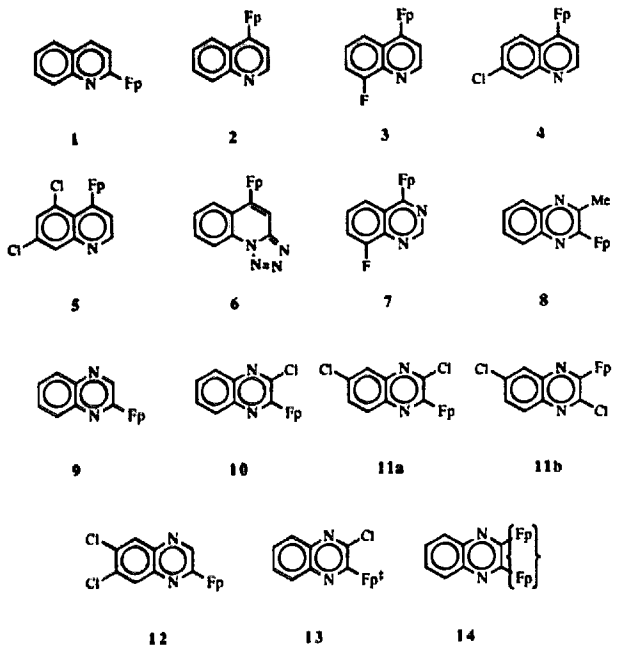

Fig. 1. Isomeric identities of the complexes (where Fp = $(C_5H_5)Fe(CO)_2$ and Fp^1 = (indenyl)$Fe(CO)_2$).

ring heterocyclic compounds containing between one and four halide substituents, e.g.

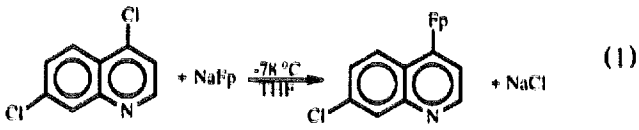

(1)

These *formal* [1–3,16] nucleophilic displacement reactions, in which the more activated chlorine atoms bonding to the nitrogen containing section of the ring are displaced by the strong Fp⁻ nucleophiles [32–34], produce a series of new polyaromatic heterocyclic products (Fig. 1). These new complexes were isolated by column chromatography in air and, except for compounds **1**, **2** and **9**, are air and moisture stable solids. Compounds **1**, **2** and **9** were isolated as oils, which slowly decomposed in this state and in solution. For complex **5**, the observed instability is not surprising since the presence of the Cl atom on the 5-position would be expected to impose a substantial steric strain (cf. the known steric effects of the *peri*-substituted tertiary butyl groups in naphthalene) [35] on the Fp group, i.e.

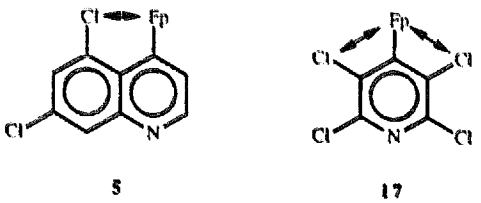

Indeed, previous attempts in our group to synthesize related compounds with *ortho*-substituted Cl and Fp groups (i.e. in **17**, above), which would be expected to show lower steric strain, were unsuccessful [1]. However, the origin of the instabilities observed for complexes **1** and **9** is not apparent, and may simply reflect the presence of trace impurities in the final oils.

Attempts to prepare *para*-substituted derivatives of monocyclic azines have previously met with failure [1,2], in spite of the fact that their arene analogues are readily prepared [4–14]. The fusion of a second arene ring onto a halogen substituted azine generally substantially increases the ease of nucleophilic substitutions. We therefore attempted to prepare a *para*-substituted phthalazine complex as a model of the related *para*-substituted heteroarene polymer. Unfortunately, no new iron–azine derivatives were isolated from the reaction of two equivalents of NaFp with 1,4-dichlorophthalazine, i.e.

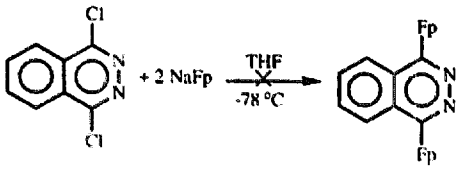

(2)

and we are therefore unable to compare the magnitude of the intermetallic conjugation in *para*-substituted arene and azine bridged complexes. In the reactions attempted involving two molar equivalents of the organometallic nucleophile and chlorinated quinoxalines, the first substitution step, e.g.

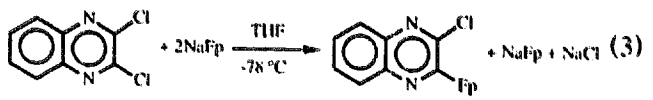

(3)

proceeds rapidly to completion, even at low temperatures, where the formation of Fp_2 is minimized. However, IR spectroscopic evidence indicates that no significant formation of the bimetallic product occurs under these conditions. If the reactants are mixed at room temperature, the formation of the disubstituted product is significant after a few minutes, but this is accompanied by concomitant formation of large amounts of the ubiquitous Fp_2 dimer. Indeed, oxidation of the Fp⁻ anion to Fp_2 always occurs in these reactions and its relative amount increases with decreased activation of the precursor azine, with decreased azine electron density, and with increased temperature [1,2,4–9]. The desired reactions are, therefore, best initiated at low

temperature, and then driven to completion in refluxing THF, i.e.

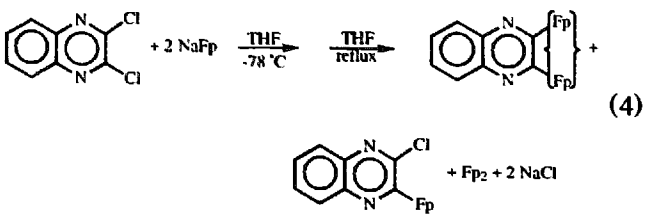

(4)

where the curly brackets around the two organometallic fragments indicate that they do not have conventional $(\eta^5\text{-}C_5H_5)Fe(CO)_2$ structures, see below. Unfortunately, even under these optimized conditions the bimetallic product is isolated in only 26% yield, and its synthesis is accompanied by the formation of both monosubstituted complexes and Fp_2 which must be removed by chromatography.

The bimetallic compounds are less air and thermally stable than the monosubstituted species, and were therefore isolated under an inert atmosphere. Interestingly, prolonged exposure of complex **14** to a Florisil filled column in air led to its decomposition by elimination of one Fp group and the introduction of a hydrogen atom in its place to give compound **9**, i.e.

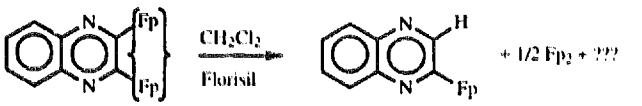

(5)

We have previously observed related decomposition reactions which seem to have a steric origin [4–9]. In fact, compound **9** was obtained exclusively via this process. To aid in unambiguously identifying the structure of complex **14**, we attempted to prepare two related derivatives, **15** and **16** (where $Fp^{\ddagger} = (\eta^5$ – indenyl)$Fe(CO)_2$), i.e.

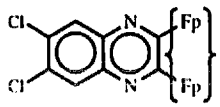

15

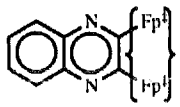

16

Unfortunately, they were even more prone to thermal decomposition and were not successfully separated from their various monometallic byproducts and Fp_2, e.g.

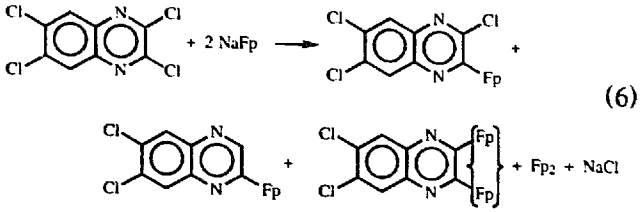

(6)

The synthesis of such *ortho*-disubstituted compounds at all was intriguing, since our earlier attempts at synthesizing related but less sterically crowded *ortho*-substituted complexes were unsuccessful, as was the attempted synthesis of the sterically crowded 2-Fp-3-phenylquinoxaline complex by the usual methods employed in this work.

3.2. Spectroscopic characterization of the complexes

The IR spectra in the carbonyl region of monosubstituted complexes **1**–**13** (Fig. 1, Table 1) are similar to those we have reported for other aryl and azinyl derivatives of Fp [1–9]. Thus, two stretching frequencies attributable to the carbonyl ligands were observed in the expected regions (i.e. a symmetric band at between 2022 and 2036 cm^{-1} and an antisymmetric band at between 1968 and 1983 cm^{-1}) [36]. The NMR data (Table 2) indicate that, with the exception of compound **11** (which is a mixture of two isomers in a 4:1 ratio), only a single isomeric complex was obtained from each of these reactions. As with other Fp containing heterocyclic compounds [1–3], the ^1H and ^{13}C NMR signals for the cyclopentadienyl rings are observed at around 5.25 ± 0.1 and 87.0 ± 0.5 ppm respectively, while the ^{13}C NMR signals for the terminal carbonyl ligands are observed at 214.64 to 216.01 ppm. (The ^{13}C NMR chemical shift for the $\eta^5\text{-}C_5H_5$ ligand in complex **5** was about 1 ppm higher than expected (i.e. 88.59), perhaps due to steric crowding between the *peri*-substituted Cl and Fp substituents on the ring.) The other ^1H and ^{13}C NMR signals for these complexes are also unexceptional, displaying the expected substituent effects due to Fp [1–9] and homonuclear and heteronuclear coupling (J_{HH} and J_{HF}) patterns consistent with the assigned structures (Fig. 1). In particular, the Fp group has characteristic influence on the chemical shifts of aromatic complexes. For example, for benzene derivatives $\Delta_{ipso} = +17.0$ ppm, $\Delta_{ortho} = +17.0$ ppm, $\Delta_{meta} = -1.0$ ppm and $\Delta_{para} = -6.0$ ppm in $(CD_3)_2SO$, while for pyrimidine derivatives with the Fp group in the 4 position the characteristic influence is $\Delta_{ipso} = +50$ ppm, Δ_{ortho}(i.e. at C5) $= +17$ ppm, Δ_{meta}(i.e. at C2) $= -12$ ppm and Δ_{meta}(i.e. at C6) $= -3$ ppm in $(CD_3)_2SO$ [1,4]. Unfortunately, these data

have not allowed an unambiguous determination of the major isomer for complex **11**. The identities of complexes **4**, **10** and **13** have also been confirmed by single crystal X-ray determinations, vide infra.

Although complexes **1** to **13** (Table 1) display the two IR bands expected [1–9] in the carbonyl region, complexes **14** and **15** display three IR bands. Two of these are observed near the expected regions (i.e. 2038 and 1992 cm^{-1} for **14**) [1–9] and the third is observed at an unusually low frequency (1928 cm^{-1} for **14** and 1938 cm^{-1} for **15** in THF) for an Fp–arene or Fp–azine complex [1–9]. These two "normal" carbonyl bands are observed at *higher* frequencies than those of the monosubstituted complexes, even though in the most closely related disubstituted species [1–9] the addition of a second Fp substituent always *decreases* the carbonyl stretching frequency by raising the electron richness of the arene or azine ring. Further, the third bands are not as low as might be expected for either conventional bridging carbonyl ligands or acyl groups. (For example, the bridging carbonyl ligands in $(\eta^5\text{-}C_5H_5)_2Fe_2(CO)_2(\mu\text{-}CO)_2$ give rise to signals at 1784 cm^{-1} (CH_2Cl_2) in the IR and around 290 ppm ($(CD_3)_2SO$) in the ^{13}C NMR, while the acyl CO group in complexes such as FP–C(O)–aryl gives rise to signals at around 1610 cm^{-1} and 255 ppm [4].) The ^1H and ^{13}C NMR spectra for compound **14** show that two different types of cyclopentadienyl group and four distinct carbonyl ligands are present in the complex, one of which (δ 219.16 ppm) is significantly deshielded from the usual values for terminal CO ligands in these complexes, vide supra, and one of which (δ 289.90 ppm) is far outside (deshielded by about 75 ppm) the usual values for terminal carbonyl ligands in such complexes, and is more typical of bridging carbonyl ligands. (For example, the bridging carbonyl ligands in $(\eta^5\text{-}C_5H_5)_2Fe_2(CO)_2(\mu\text{-}CO)_2$ give rise to signals at 1784 cm^{-1} (CH_2Cl_2) in the IR and around 290 ppm ($(CD_3)_2SO$) in the ^{13}C NMR, while the acyl CO group in complexes such as FP–C(O)–aryl gives rise to signals at around 1610 cm^{-1} and 255 ppm [4].) In addition to a "normal", vide supra, cyclopentadienyl ligand (giving rise to ^1H and ^{13}C NMR signals at 5.22 and 87.81 ppm respectively) [1–9], unusually high field signals (at 4.84 ppm for ^1H and 82.86 ppm for ^{13}C NMR) are also observed in 1:1 intensity ratios. In addition, the ^1H and ^{13}C NMR spectra of complex **14** indicate that the quinoxaline ring is unsymmetrical. Taken together, these spectroscopic data unambiguously indicate that complex **14** does not have two conventional $(\eta^5\text{-}C_5H_5)Fe(CO)_2$ substituents. Rather, we propose that it may have one terminal and one bridging $\eta^5\text{-}C_5H_5$ ligand and three terminal (one of which is in an unusual chemical environment for an Fp–R complex) and one (semi)bridging carbonyl ligand. Such a bridging cyclopentadienyl ligand [37] would account for the unusual ^1H and ^{13}C NMR signals of this steriochemically non-rigid group (no evidence for the "freezing out" of any of these resonances at temperatures down to −80 °C was observed), while a "bridging" carbonyl would also account for the low field ^{13}C NMR signals and the low energy carbonyl band in the IR [38–40].

Unfortunately, our attempts to unambiguously determine these structures by X-ray crystallographic analysis of complexes **14** and **15** have been unsuccessful due to our inability to obtain single crystals of these complexes. Hence, we attempted to prepare (cf. Eq. (4)) analogues of **14** and **15** with $(\eta^5\text{-indenyl})Fe(CO)_2$, Fp^*, groups rather than the more sterically demanding $(\eta^5\text{-cyclopentadienyl})Fe(CO)_2$, Fp, groups. Unfortunately, these efforts were also unsuccessful, producing a monometallic species, **13**, rather than the desired bimetallic complex, **16**, as the only well characterized product. Thus, any suggestion of the detailed structures of bimetallic complexes **14** and **15** must remain tentative until the X-ray analysis of one of them or one of their analogues can be carried out.

3.3. X-ray crystal structures of complexes 4, 10 and 13

The X-ray structure determinations of the title complexes (Table 3, Tables 7–9) confirmed that they have the substitution geometries proposed on the basis of spectroscopic evidence (Fig. 1). Thus, for the quinoline

Table 7
Selected bond lengths (Å) and angles (°) for complex **4** [a]

Fe–C11	2.004(8)	C11–C12	1.41(1)	C15–C16	1.39(1)
Fe–C(Cp)	2.10(av.)	C12–C13	1.38(1)	C16–C17	1.37(1)
Fe–C1	1.78(1)	C13–N14	1.31(1)	C17–C18	1.37(1)
Fe–C2	1.746(9)	N14–C19	1.38(1)	C15–C19	1.41(1)
C1–O1	1.14(1)	C19–C20	1.43(1)	C18–C20	1.41(1)
C2–O2	1.142(9)	C11–C20	1.42(1)	Cl–C16	1.735(8)
C1–Fe–C2	90.4(4)	Fe–C1–O1	177.5(8)	Fe–C11–C20	125.5(6)
C1–Fe–C11	90.6(4)	Fe–C2–O2	176.1(9)	Cl–C16–C15	118.5(7)
C2–Fe–C11	92.9(4)	Fe–C11–C12	118.2(6)	Cl–C16–C17	120.2(7)

[a] Numbers in parentheses are estimated standard deviations in the least significant digit.

Table 8
Selected bond lengths (Å) and angles (°) for complexes **10** and **13** [a]

Length/angle	10	13	Length/angle	10	13
Fe–C2	1.975(2)	1.973(2)	C6–C7	1.403(4)	1.406(4)
Fe–C21	1.766(2)	1.765(3)	C7–C8	1.357(3)	1.361(4)
Fe–C22	1.769(2)	1.765(3)	C8–C9	1.415(2)	1.401(4)
C21–O21	1.140(2)	1.145(4)	C9–C10	1.400(3)	1.405(3)
C22–O22	1.142(2)	1.148(4)	C5–C10	1.406(3)	1.399(3)
N1–C2	1.318(2)	1.310(3)	Fe–C(Cp)	2.107(av.)	—
C2–C3	1.452(2)	1.455(3)	Fe–C11	2.116(2)	2.183(2)
Cl–C3	1.750(3)	1.752(2)	Fe–C12	2.095(2)	2.093(3)
C3–N4	1.289(2)	1.288(3)	Fe–C13	2.107(2)	2.089(2)
N1–C9	1.370(2)	1.373(4)	Fe–C14	2.106(2)	2.111(3)
N4–C10	1.372(2)	1.374(4)	Fe–C15	2.125(2)	2.182(2)
C5–C6	1.369(3)	1.366(3)			
C21–Fe–C22	93.22(9)	95.7(2)	C2–N1–C9	120.6(2)	120.5(2)
C2–Fe–C21	95.65(8)	93.8(1)	N1–C9–C10	121.3(2)	120.9(2)
C2–Fe–C22	87.82(8)	87.4(1)	Cl–C3–N4	114.5(1)	114.4(1)
Fe–C21–O21	176.8(2)	176.7(3)	Cl–C3–C2	118.9(1)	119.4(1)
Fe–C22–O22	179.3(2)	178.4(3)	N4–C3–C2	126.6(2)	126.2(2)
Fe–C2–N1	118.0(1)	118.4(2)	C3–N4–C10	116.5(2)	116.5(2)
Fe–C2–C3	126.2(1)	125.6(1)	N4–C10–C9	119.6(2)	119.9(2)
N1–C2–C3	115.3(2)	116.0(2)			

[a] Numbers in parentheses are estimated standard deviations in the least significant digit.

derivative **4**, the nucleophilic substitution reaction occurred at carbon 4 of the aromatic ring bearing the nitrogen heteroatom (Table 7 and Fig. 2). This structure is similar to that of anti-malarial agents such as Chloroquine [18–22], except that the σ- and π-electron donating Fp substituent replaces the more strongly π-electron donating, but σ-electron withdrawing, NR_2 substituents in the purely organic agents. In complex **4**, the Fp substituent retains the conventional three-legged piano stool geometry and the Fe–C11 bond distance (i.e. 2.004(8) Å) is similar to that in related Fp–azine complexes having formal Fe–C single bonds [1–3,5]. The most chemically interesting features of this structure are the observed C20–C11–Fe (125.5(6)°) and C12–C11–Fe (118.2(6)°) angles and the relatively short H18–Fe contact distance (2.98 Å), which are consistent with the proposed steric interaction between the *peri*-substituents in the related, but even more crowded, complex **5**, vide supra.

The two monometallic quinoxaline derivatives having η^5-cyclopentadienyl, **10**, and η^5-indenyl, **13**, ligands on iron have very similar X-ray crystal structures (Tables 8 and 9 and Fig. 3 and Fig. 4). Thus, complex **10** has a conventional Fp group with a symmetric

Table 9
Least squares plane containing quinoxaline rings for complexes **10** and **13** [a]

Complex	Coefficients [b]	Defining atoms with deviations [c]			
10	3.5876, −5.6230, 5.3905, −0.0249	N1	0.019(2)	C2	0.030(2)
		C3	−0.032(2)	N4	−0.020(2)
		C5	0.032(2)	C6	0.040(3)
		C7	−0.034(2)	C8	−0.050(3)
		C9	−0.007(2)	C10	0.010(2)
		Fe	0.357	*Cl*	−0.120
13	9.9028, −5.5345, 1.4759, 2.5029	N1	0.007(2)	C2	−0.016(3)
		C3	0.020(3)	N4	0.014(2)
		C5	−0.021(3)	C6	−0.013(3)
		C7	0.014(3)	C8	0.026(3)
		C9	−0.002(3)	C10	−0.006(3)
		Fe	−0.157	*Cl*	0.029

[a] Weights are derived from the atomic positional e.s.d.s using the method of Hamilton, *Acta Crystallogr.*, *14* (1961) 185.
[b] Coefficients are for the form $ax + by + cz - d = 0$ where x, y and z are crystallographic coordinates.
[c] Deviations are in angstroms with the e.s.d. given in parentheses. Underlined atoms were not included in the definition of the plane.

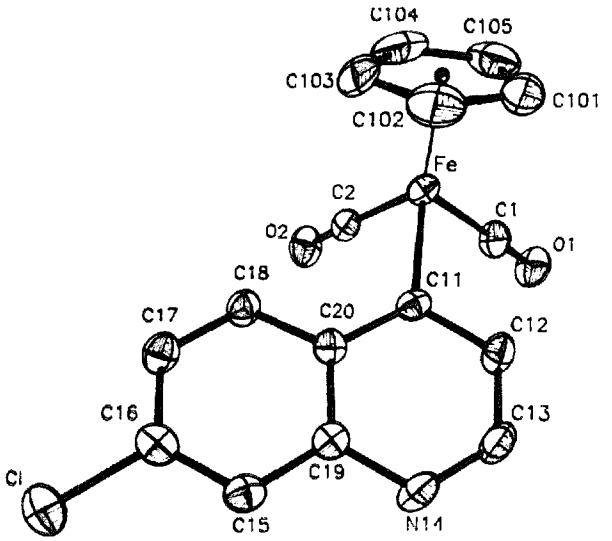

Fig. 2. ORTEP plot for 4-[(η^5-cyclopentadienyl)irondicarbonyl]-7-chloroquinoline **4**.

η^5-cyclopentadienyl ligand and normal Fe–CO, FeC–O, and Fe–azine bond lengths and angles [1–3,5]. Its η^5-indenyl analogue, **13**, has similar bond lengths and angles, as would be expected based on their spectral properties (Tables 1 and 2). The η^5-indenyl ligand shows the expected slippage of the five-membered ring to produce three shorter (2.089(2), 2.111(3) and 2.093(3) Å) and two longer (2.182(2) and 2.183(2) Å) metal–indenyl bonds [41]. The most chemically interesting features of these structures are the structural distortions that they display, i.e.

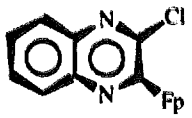

These are apparently due to repulsive steric interactions between their organometallic substituents in the 2 positions and the chloro substituents in the 3 positions of the ring (Table 4 and Fig. 3(b)). Thus, the observed Fe–C2–C3 angles for **10** and **13** are 126.2(1) and 125.6(1)° respectively, and the Fe–C2–C3–C1 torsion angles in complexes **10** and **13** are 11.95(27) and 3.67(34)° respectively. Interestingly, the degree of this steric distortion is significantly smaller for complex **13**, having the less sterically demanding η^5-indenyl ligand. Based on the structures of monometallic complexes **10** and **13**, it appears that steric strain between two *ortho*-substituted organometallic fragments in complexes **14** and **15** would be very large if their Fp substituents were not bonded to one another, e.g.

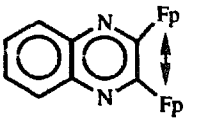

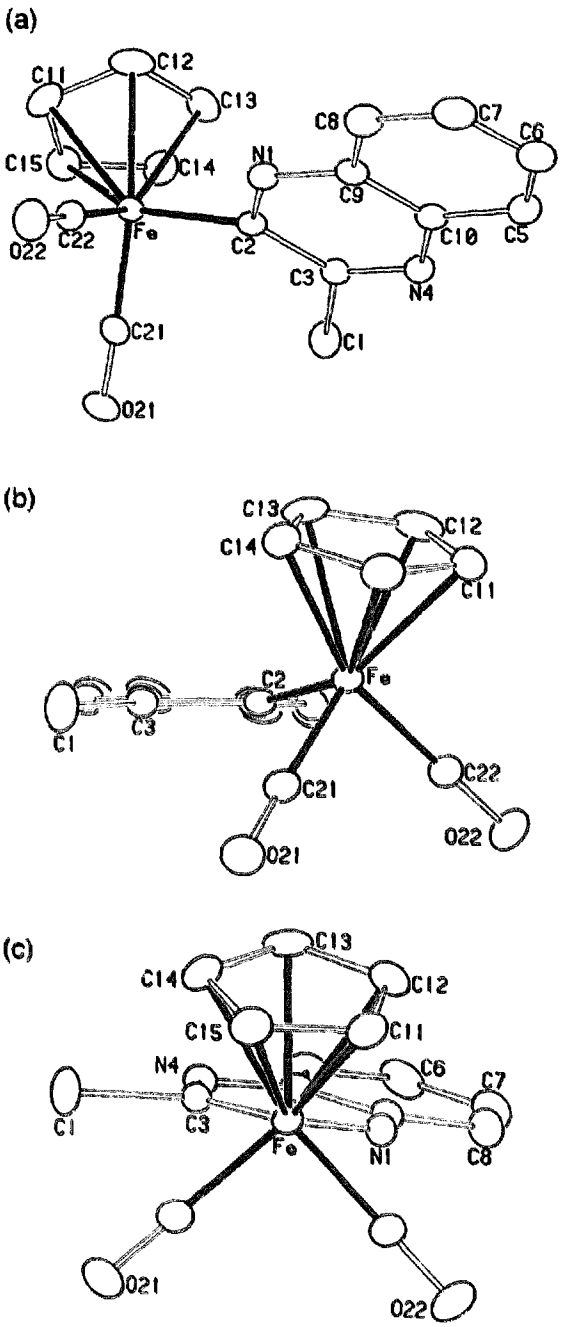

Fig. 3. ORTEP plots for 2-[(η^5-cyclopentadienyl)irondicarbonyl]-3-chloroquinoxaline **10**: (a) perspective view, (b) view in the azine ring plane, and (c) view down the Fe–C2 bond.

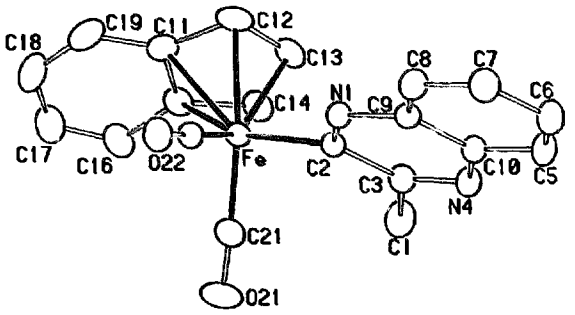

Fig. 4. ORTEP plot for 2-[(η^5-indenyl)irondicarbonyl]-3-chloroquinoxaline **13**.

Indeed, we calculate Fe–Fe distances in such species of about 3.5 Å if they have conventional Fp substituents and bond lengths and angles similar to their monometallic analogues **10** and **13**. This predicted Fe–Fe distance is substantially less than the sum of the Van der Waals radii (i.e. about 4.0 Å) supporting our proposal that they may have some more direct covalent interaction. (In a recent paper the Van der Waal's radius of iron atoms is given as 2.03 Å [42]. Alternatively, the Van der Waal's radius of the iron atom in the $CpFe(CO)_2$ fragment can also be estimated as being equal to its covalent radius plus about 0.76 to 0.80 Å [43,44] (i.e. in these complexes the value for Fe is around 1.25 + 0.78 = 2.03 Å).)

Finally, it is worth commenting that in each of these complexes the Fp or Fp^* substituents adopt conformations in which their pseudo mirror planes are approximately perpendicular to the plane of the azine (i.e. Fig. 3(c)). As with the other related arene and azine derivatives that we have crystallographically characterized, these conformations are the opposite to those predicted on molecular orbital grounds and are likely adopted to minimize adverse steric interactions between the H atoms on the Cp or Cp^* ligands and the atoms *peri*- or *ortho*-substituted to the metal [1–9,45–47].

4. Conclusions

A series of 14 new monometallic derivatives of quinoline, quinoxaline, quinazoline and tetraazolo(1,5-A)quinoline has been prepared and characterized. Possible structures of the bimetallic derivatives of quinoxaline having *ortho*-substituted organometallic centers, which exhibit unusual IR and NMR spectral properties consistent with bridging carbonyl and cyclopentadienyl ligands, have also been discussed. X-ray crystallographic characterization of representative quinoline and quinoxaline complexes confirms that they have the proposed structures and emphasizes the importance of steric effects in determining their detailed geometries. The structures of many of these derivatives are similar to those of related biologically active materials, including herbicides, fungicides, and insecticides, and we are attempting to determine if the organometallic complexes will also display significant biological activities. (The results of the biological screening tests for representative examples of these complexes (as herbicides, fungicides and insecticides) will be published as part of a separate manuscript.)

5. Supplementary material available

For enquiries concerning the structural determination of complexes **10** and **13** contact B.D.S. quoting ADH.8906 and ADH.9110 respectively.

Complete descriptions of the X-ray crystal structure determinations, tables of atomic coordinates and anisotropic Gaussian parameters, bond lengths, bond angles, hydrogen atom coordinates and Gaussian parameters, least squares planes, torsional angles, root-mean-square amplitudes of vibration (35 pages) for the three crystal structures and structure factor amplitudes (58 pages) for the three crystal structures are available from the authors.

Acknowledgements

The authors would like to acknowledge Youngstown State University and its University Research Council (A.D.H.), DowElanco of Greenfield Indiana (R.C. and A.D.H.), the Natural Sciences and Engineering Research Council of Canada (R.C., A.D.H., and B.D.S.), and the National Science Foundation (S.G.B. and J.L.A.) for their financial support of this work. A.D.H. would also like to thank the National Science Foundation (DMR Grant No. 9403889), the Ohio Board of Regents, and Youngstown State University for funds used to purchase the Siemens diffractometers located in the Youngstown State University Structure Center. We would also like to thank Eli Lilly and Co. and DowElanco for supplying some of the heteroaromatic starting materials used in this work and Dr. R. McDonald of the University of Alberta Structure Determination Laboratory for his assistance.

References

[1] R. Chukwu, A.D. Hunter and B.D. Santarsiero, *Organometallics*, *10* (1991) 2141–2152.

[2] R. Chukwu, A.D. Hunter, B.D. Santarsiero, S.G. Bott, J.L. Atwood and J. Chassaignac, *Organometallics*, *11* (1992) 589–597.

[3] R. Chukwu, X.A. Guo, A.D. Hunter, B.D. Santarsiero and S.G. Bott, in preparation.

[4] A.D. Hunter and A.B. Szigety, *Organometallics*, *8* (1989) 2670–2679.

[5] A.D. Hunter and J.L. McLernon, *Organometallics, 8* (1989) 2679–2688.
[6] G.B. Richter-Addo and A.D. Hunter, *Inorg. Chem., 28* (1989) 4063–4065.
[7] G.B. Richter-Addo, A.D. Hunter and N. Wichrowska, *Can. J. Chem., 68* (1990) 41–48.
[8] A.D. Hunter, D. Ristic-Petrovic and J.L. McLernon, *Organometallics, 11* (1992) 864–871.
[9] J. Li, A.D. Hunter, R. McDonald, B.D. Santarsiero, S.G. Bott and J.L. Atwood, *Organometallics, 11* (1992) 3050–4055.
[10] R. McDonald, K.C. Sturge, A.D. Hunter and L. Shilliday, *Organometallics, 11* (1992) 893–900.
[11] K.C. Sturge, A.D. Hunter, R. McDonald and B.D. Santarsiero, *Organometallics, 11* (1992) 3056–3062.
[12] P.M. Macdonald, A.D. Hunter, G. Lesley and J. Li, *J. Solid State Nucl. Magn. Reson., 2* (1993) 47–55.
[13] X.A. Guo, K.C. Sturge, A.D. Hunter and M.C. Williams, *Macromolecules, 27* (1994) 7825–7829.
[14] X.A. Guo, A.D. Hunter and J. Chen, *J. Polym. Sci. A: Polym. Chem., 32* (1994) 2859–2866.
[15] P.N. Prasad and D.R. Ulrich, *Non-linear Electroactive Polymers*, Plenum, New York, 1988.
[16] R. Chukwu, *M.Sc. Thesis*, The University of Alberta, 1990.
[17] F.R. Benson, *High Nitrogen Compounds*, Wiley, New York, 1984, pp. 403–414.
[18] M. Windholz (ed.), *The Merck Index*, Merck and Co., Rahway, 10th edn., 1983.
[19] H.G. Franck and J.W. Stadelhofer, *Industrial Aromatic Chemistry*, Springer, New York, 1987.
[20] R.B. Silverman, *The Organic Chemistry of Drug Design and Drug Action*, Academic Press, New York, 1992.
[21] M.B. Green, G.S. Hartley and T.F. West, *Chemicals for Crop Improvement and Pest Management*, Pergamon, New York, 1987.
[22] R.J. Cremlyn, *Agrochemicals*, Wiley, New York, 1991.
[23] D.F. Shriver and M.A. Drezdzon, *The Manipulation of Air-Sensitive Compounds*, Wiley, New York, 2nd edn., 1986.
[24] D.D. Perrin, W.L.F. Armarego and D.R. Perrin, *The Purification of Laboratory Chemicals*, Pergamon, New York, 2nd edn., 1980.
[25] R.B. King and J. Eisch, *Organomet. Synth., 1* (1965) 114.
[26] T.C. Forschner and A.R. Cutler, *Inorg. Chim. Acta, 102* (1985) 113–120.
[27] J. Holton, M.F. Lappert, D.G.H. Ballard, R. Pearce, J.L. Atwood and W.E. Hunter, *J. Chem. Soc., Dalton Trans.*, (1979) 45.
[28] G.M. Sheldrick, in G.M. Sheldrick, C. Kruger and R. Goddard (eds.), *Crystallographic Computing 3*, Oxford University Press, London, 1985, pp. 175–189.
[29] G.M. Sheldrick, SHELX-76, *A System of Computer Programs for X-Ray Structure Determination*, Cambridge University Press, Cambridge, 1976.
[30] The diffractometer programs are those supplied by Enraf-Nonius for operating the CAD4F diffractometer, some modifications by Dr. R.G. Ball at the University of Alberta. *International Tables for X-ray Crystallography*, Vol. I, Kynoch Press, Birmingham, 1974. The computer programs used in this analysis include the Enraf-Nonius Structure Determination Package, Vers. 3, 1985, Delft, adapted for a SUN Microsystems 3/160 computer, and several programs written by Dr. R.G. Ball at the University of Alberta. *International Tables for X-ray Crystallography*, Vol. IV, Kynoch Press, Birmingham, 1974, tables 2.2B and 2.3.1 (present distributor: Reidel, Dordrecht). N. Walker and D. Stuart, *Acta Crystallogr., A39* (1983) 158.
[31] J.V. Metzzer (ed.), *Heterocyclic Compounds*, Vol. 34, Wiley, New York, 1979, p. 568.
[32] R.E. Dessy, R.L. Pohl and R.B. King, *J. Am. Chem. Soc., 88* (1966) 5121–5124.
[33] S. Henderson and R.A. Henderson, *Adv. Phys. Org. Chem., 23* (1987) 1–62.
[34] G.A. Artamkina, A.Y. Mil'Chenko, I.P. Beletskaya and O.A. Reutov, *J. Organomet. Chem., 311* (1986) 199–206.
[35] W.J. Le Noble, in P.G. Gassman (ed.), *Highlights of Organic Chemistry, An Advanced Textbook*, Vol. 3, Marcel Dekker, New York, 1974, pp. 224–225.
[36] F.A. Cotton and C.S. Kraihanzel, *J. Am. Chem. Soc., 84* (1962) 4432.
[37] C.M. Lukehart, *Fundamental Transition Metal Organometallic Chemistry*, Brooks/Cole, Monterey, CA, 1985, p. 112.
[38] C.M. Lukehart, *Fundamental Transition Metal Organometallic Chemistry*, Brooks/Cole, Monterey, CA, 1985, pp. 102–103.
[39] M.A. Greaney, J.S. Merola and T.R. Halbert, *Organometallics, 4* (1985) 2057–2058.
[40] M.D. Curtis, K.B. Shiu, W.M. Butler and J.C. Huffman, *J. Am. Chem. Soc., 108* (1986) 3335–3343 and references cited therein.
[41] A.K. Kakkar, S.F. Jones, N.J. Taylor, S. Collins and T.B. Marder, *J. Chem. Soc., Chem. Commun.*, (1989) 1454–1456 and references cited therein.
[42] K. Nagle, *J. Am. Chem. Soc., 112* (1990) 4741.
[43] A. Bondi, *J. Phys. Chem., 68* (1964) 441.
[44] L. Pauling, *The Nature of the Chemical Bond*, Cornell University Press, Ithica, NY, 3rd edn., 1960, p. 263.
[45] B.E.R. Schilling, R. Hoffmann and J.W. Faller, *J. Am. Chem. Soc., 101* (1979) 592–598.
[46] J.I. Seeman and S.G. Davies, *J. Am. Chem. Soc., 107* (1985) 6522–6531.
[47] G.L. Crocco and J.A. Gladysz, *J. Am. Chem. Soc., 110* (1988) 6110–6118 and references cited therein.